

Accepted Manuscript

Heterocyclic thioamide/phosphine mixed-ligand silver(I) complexes: Synthesis, molecular structures, DNA-binding properties and antibacterial activity

Despoina Varna, Eleni Kapetanaki, Alexandra Koutsari, Antonios G. Hatzidimitriou, George Psomas, Panagiotis Angaridis, Rigini Papi, Anastasia A. Pantazaki, Paraskevas Aslanidis

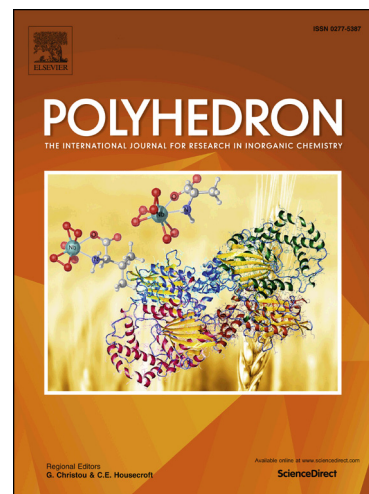
PII: S0277-5387(18)30258-4
DOI: <https://doi.org/10.1016/j.poly.2018.05.020>
Reference: POLY 13167

To appear in: *Polyhedron*

Received Date: 13 March 2018
Accepted Date: 9 May 2018

Please cite this article as: D. Varna, E. Kapetanaki, A. Koutsari, A.G. Hatzidimitriou, G. Psomas, P. Angaridis, R. Papi, A.A. Pantazaki, P. Aslanidis, Heterocyclic thioamide/phosphine mixed-ligand silver(I) complexes: Synthesis, molecular structures, DNA-binding properties and antibacterial activity, *Polyhedron* (2018), doi: <https://doi.org/10.1016/j.poly.2018.05.020>

This is a PDF file of an unedited manuscript that has been accepted for publication. As a service to our customers we are providing this early version of the manuscript. The manuscript will undergo copyediting, typesetting, and review of the resulting proof before it is published in its final form. Please note that during the production process errors may be discovered which could affect the content, and all legal disclaimers that apply to the journal pertain.



Heterocyclic thioamide/phosphine mixed-ligand silver(I) complexes: Synthesis, molecular structures, DNA-binding properties and antibacterial activity

Despoina Varna,^a Eleni Kapetanaki,^a Alexandra Koutsari,^a Antonios G. Hatzidimitriou,^a George Psomas,^a Panagiotis Angaridis,^{*a} Rigini Papi,^b Anastasia A. Pantazaki^b and Paraskevas Aslanidis^a

^a*Laboratory of Inorganic Chemistry, Department of Chemistry, Aristotle University of Thessaloniki, Thessaloniki 541 24, Greece*

^b*Laboratory of Biochemistry, Department of Chemistry, Aristotle University of Thessaloniki, Thessaloniki 541 24, Greece*

Synopsis:

Silver(I) complexes with heterocyclic thioamides (or thioamidates) and phosphine ligands, with either tetrahedral or trigonal planar coordination geometries have been synthesized and structurally characterized. Their CT DNA binding affinity and antibacterial activity has been examined.

Dedicated to Prof. Spyros P. Perlepes on the occasion of his 65th birthday

* Corresponding author:

Tel.: +30 2310 99 7437. E-mail address: panosangaridis@chem.auth.gr (P. Angaridis).

ACCEPTED MANUSCRIPT

ABSTRACT

Five silver(I) mixed-ligand complexes containing a heterocyclic thioamide (mtdztH = 5-methyl-1,3,4-thiadiazole-2-thiol or atdztH = 5-amino-1,3,4-thiadiazole-2-thiol or mqztH = 2-mercapto-4(3H)-quinazolinone) and triphenylphosphine (PPh_3) have been synthesized and structurally characterized. Four of these compounds, namely $[\text{AgCl}(\text{PPh}_3)_2(\text{mtdztH})]$ (**1**), $[\text{AgCl}(\text{PPh}_3)_2(\text{mqztH})]$ (**2**), $[\text{Ag}(\text{PPh}_3)_3(\text{mtdzt})]$ (**3**) and $[\text{Ag}(\text{PPh}_3)_3(\text{atdzt})]$ (**4**) reveal a distorted tetrahedral coordination environment, while $[\text{Ag}(\text{PPh}_3)_2(\text{atdzt})]$ (**5**) adopts a trigonal planar arrangement. The interaction of the compounds with calf-thymus DNA was monitored via UV-vis spectroscopy, DNA-viscosity measurements and their competition with ethidium bromide for the DNA-intercalation sites studied by fluorescence emission spectroscopy. The affinity of all the silver(I) complexes for the interaction with CT DNA is high and takes place via an intercalative mode. The new complexes show *in vitro* antibacterial activity against certain Gram-positive (*Bacillus subtilis*, *Bacillus cereus*, *Staphylococcus aureus*) bacterial strains, but are inactive against the Gram-negative *Escherichia coli*. Interestingly, higher activity was detected for the trigonal planar compound compared to its tetrahedrally coordinated counterparts.

keywords: Silver(I); heterocyclic thioamides; Crystal structures; Interaction with DNA; Antimicrobial activity

1. INTRODUCTION

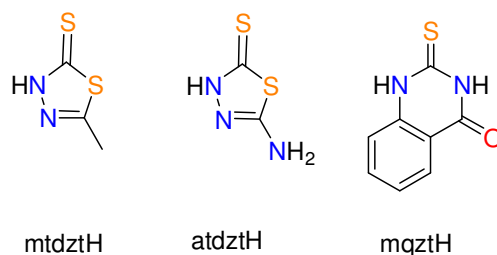
During the last few decades, coordination compounds bearing heterocyclic thioamide ligands have attracted much research interest [1]. The ability of these molecules to coordinate metal centers in a monodentate or a bridging mode, resulted in the synthesis of a large variety of compounds, among them a significant number of copper(I) and silver(I) complexes bearing bulky triarylphosphines as auxiliary ligands. The vast majority of these complexes reveal a tetra-coordinate monomeric or dimeric nature, although there are some examples of three-coordinate species, particularly in the presence of bulky triarylphosphines [2]. The interest for much of the research into the coordination chemistry of heterocyclic thioamides stems, however, from their close relevance to biological system [3]. In fact, they are regarded as a very promising starting point for biological studies and transition metal complexes of several imidazole-, thiazole-, oxazole-, and uracil-based derivatives have been the subject of investigations towards pharmacological activities [4].

Silver salts are known for long time for their effectiveness as antiseptic, antibacterial and anti-inflammatory agents and were widely used until the appearance of antibiotics. Nowadays, with the increasing resistance of bacteria to antibiotics, research has turned significantly towards developing of silver coordination compounds with improved pharmacological characteristics [5]. At the same time, much attention has also been paid to the antitumor and anti-proliferative characteristics of silver(I) complexes a particular intense activity on the antitumor and anti-proliferative activity of silver(I) complexes is also in progress [6], whereby the status of the respective investigations has being reviewed recently [7].

For quite a long time, research in our laboratory largely focused on heterocyclic thioamide/phosphine mixed-ligand copper(I) and silver(I) complexes, with the aim to understand the factors affecting the stoichiometric and structural preferences of these compounds. Considering silver(I) complexes bearing neutral heterocyclic thioamides and

triphenylphosphine (PPh_3), the majority of the examples isolated and structurally characterized in our laboratory so far consist both of monomeric species exhibiting a tetrahedral or trigonal environment around the metal centre [8] and doubly S-bridged symmetric dimmers [9]. Meanwhile, many of these compounds have been proven to show interesting antimicrobial and biological activity; thus, we decided to look for possible relationships between structure and bioactivity. For example, in a recent report we presented two series of copper(I) halide complexes of N-methylbenzothiazole-2-thione (abbreviated as mbtt), namely dinuclear $[\text{CuX}(\text{mbtt})_2]_2$ and mononuclear $[\text{CuX}(\text{PPh}_3)_2(\text{mbtt})]$, of which only the later showed significant antibacterial activity against several Gram-positive and Gram-negative microorganisms [10]. Further, a remarkably high antibacterial activity was found for the mononuclear $[\text{CuI}(\text{xantphos})(\text{mbtt})]$ (xantphos=4,5-bis(diphenylphosphino)-9,9-dimethyl-xanthene) [11]. As for the analogous silver(I) complexes, it has been found that they are more active than the corresponding copper(I) compounds [12].

Based on this background, we decided to gain more insight into the relationship between the molecular structures of heterocyclic thioamide/phosphine mixed-ligand silver(I) complexes and their bioactivity. In particular, herein we report the synthesis of five new neutral silver(I) complexes bearing specific combinations of heterocyclic thioamides (or thioamidates), shown in Scheme 1, and a varying number of PPh_3 ligands in their coordination sphere, in the presence (or absence) of a coordinated halide ion, and to study the effect the nature of particular thioamide ligands and the different coordination environments of the complexes, on their interaction with calf-thymus (CT) DNA as well their antimicrobial properties.



Scheme 1. Heterocyclic thioamides used in this work

2. EXPERIMENTAL

2.1 General procedures and chemicals

All manipulations were carried out under atmospheric conditions, unless otherwise mentioned. Solvents were purified according to established methods and allowed to stand over molecular sieves for 24 h. Silver(I) starting materials, i.e. silver chloride (AgCl), silver tetrafluoroborate (AgBF₄), silver nitrate (AgNO₃), the thioamides 5-methyl-1,3,4-thiadiazole-2(3H)-thione (mtdztH), 5-amino-1,3,4-thiadiazole-2(3H)-thione (atdztH) and 2-mercapto-4(3H)-quinazolinone (mqztH), triphenylphosphine (PPh₃), CT DNA, ethidium bromide (EB), NaCl and trisodium citrate CT DNA, ethidium bromide (EB), NaCl and trisodium citrate were obtained from commercial sources and used without any further purification.

DNA stock solution was prepared by dilution of CT DNA to buffer (containing 15 mM trisodium citrate and 150 mM NaCl at pH 7.0) followed by vigorous stirring for three days, and kept at 4°C for no longer than a week. This solution of CT DNA gave a ratio of UV absorbance at 260 and 280 nm (A_{260}/A_{280}) of ~1.90, indicating that the DNA was sufficiently free of protein contamination [13]. The DNA concentration was determined by the UV absorbance at 260 nm after 1:20 dilution using $\epsilon = 6600 \text{ M}^{-1}\text{cm}^{-1}$ [14].

2.2 Syntheses

2.2.1 [AgCl(PPh₃)₂(κ -S-mtdztH)], **1**

To a suspension of AgCl (0.072 g, 0.5 mmol) in 25 mL of CH₃CN, PPh₃ (0.262 g, 1.0 mmol) was added in small portions. The resulting mixture was stirred at 50°C for 24 h in dark and then an amount of 0.066 g (0.5 mmol) of mtdztH was added. The reaction mixture was further stirred at 60°C for 2 h in dark and then it was allowed to cool at room temperature. After filtering the reaction mixture, the filtrate was set aside in dark to evaporate slowly at room temperature and, over a period of 24 h, large crystals of **1** were grown which were collected. Yield: 0.152 g (38%). Anal. Calcd for C₃₉H₃₄AgClN₂P₂S₂: C, 58.54; H, 4.28; N, 3.50. Found: C, 58.24; H, 4.52; N, 3.71. FTIR (KBr, cm⁻¹): 3044w, 2955w, 1552m, 14777vs, 1432vs, 12774vs, 1198m, 1097vs, 1049vs, 1024m, 998m, 748vs, 694vs, 504vs, 489vs. UV-Vis (CH₃CN), λ /nm (log ϵ): 256 (3.66), 310 (4.03).

2.2.2 [AgCl(PPh₃)₂(κ -S-mqztH)], **2**

A portion of 0.072 g (0.5 mmol) of AgCl was suspended in 20 mL of CH₃CN and then PPh₃ (0.262 g, 1.0 mmol) was added. The resulting mixture was stirred at 50°C for 18 h in dark and then a solution of mqztH (0.089 g, 0.5 mmol) in 20 mL of MeOH was added dropwise. The reaction mixture was stirred at 60°C for 3 h in dark and, after allowing it to cool at room temperature, it was filtered. The filtrate was set aside in dark to evaporate slowly at room temperature and, over a period of 5 days, crystals of **2** were grown which were collected. Yield: 0.178 g (42%). Anal. Calcd for C₄₄H₃₆AgClN₂OP₂S: C, 62.46; H, 4.29; N, 3.31. Found: C, 62.21; H, 4.46; N, 3.48. FTIR (KBr, cm⁻¹): 3050m, 2968w, 1680vs, 1615vs, 1552vs, 1479vs, 1420s, 1306m, 1267s, 1159vs, 1095s, 996m, 744vs, 515s, 503vs, 409s. UV/Vis (CH₃CN), λ /nm (ϵ): 250 (4.32), 291 (4.36).

2.2.3 [Ag(κ -S-mtdzt)(PPh₃)₃], **3**

A portion of AgBF₄ (0.097 g, 0.5 mmol) was dissolved in a 10-mL mixture of CH₃CN:MeOH (1:1 v/v) and then PPh₃ (0.262 g, 1.0 mmol) was added in small portions. The resulting mixture was stirred at 50°C for 20 min in dark and then a 20-mL methanolic solution of mtdzt in the same solvent mixture, obtained from the deprotonation of the corresponding amount of mtdztH (0.066 g, 0.5 mmol) with 1.0 mL of 0.5 M solution of KOH in MeOH, was added dropwise. After stirring at 65°C for 1 h, the resulting suspension was filtered in order to remove a small amount of an off-white solid. The filtrate was set aside in dark to evaporate slowly at room temperature and, after 5 days, crystals of **3** started growing, which were collected. Yield: 0.300 g (57%). Anal. Calcd for C₅₈H₅₂AgN₂OP₃S₂: C, 65.85; H, 4.95; N, 2.65. Found: C, 66.01; H, 4.70; N, 2.83. FTIR (KBr, cm⁻¹): 3448br, 3052w, 1579m, 1481s, 1437vs, 1368m, 1307m, 1281w, 1179s, 1087s, 996s, 743vs, 698vs, 516vs, 500vs. UV/Vis (CH₃CN), λ /nm (ϵ): 250 (4.32), 291 (4.36). UV/Vis (CH₃CN), λ /nm (ϵ): 257 (4.34).

2.2.4 [Ag(κ -S-atdzt)(PPh₃)₃], **4**

To a 20-mL mixture of CH₃CN/MeOH (1:1 v/v) portions of AgNO₃ (0.085 g, 0.5 mmol) and PPh₃ (0.262 g, 1.0 mmol) were added and the resulting suspension was stirred at mild temperature (~50°C) for 24 h in dark. Next, a 10-mL solution of amtdz, obtained by addition of 1.0 mL of a 0.5 M methanolic solution of KOH into a solution of amtdztH (0.066 g, 0.5 mmol) in the same solvent mixture, was added. After stirring the reaction mixture at 50°C for 2 h in dark, it was filtered in order to remove a small amount of an off-white solid, and the filtrate was set aside in dark to evaporate slowly at room temperature. After 3 days, crystals of **4** were grown, which were collected. Yield: 0.272 g (51%). Anal. Calcd for C₅₈H₅₀AgN₄P₃S₂: C, 65.23; H, 4.72; N, 5.25. Found: C, 65.04; H, 4.85; N, 5.38. FTIR (KBr,

cm⁻¹): 3054m, 1617m, 1585m, 1478vs, 1308m, 1091s, 1026m, 997m, 745vs, 694vs, 513vs, 501vs. UV/Vis (CH₃CN), λ /nm (ϵ): 260 (4.65), 314 (3.09).

2.2.5 [Ag(κ -S-atdzt)(PPh₃)₂], **5**

To a 10-mL mixture of CH₃CN/MeOH (1:1 v/v), the amount of 0.072 g (0.5 mmol) of AgCl was added. Next, a solution of PPh₃ (0.262 g, 1.0 mmol) in 10 mL of the same solvent mixture was added. The resulting mixture was stirred at 50°C for 20 min in dark and then a 10-mL solution of amtdzt in MeOH, which was obtained after deprotonation of amtdztH (0.066 g, 0.5 mmol) by 1.0 mL of a 0.5 M solution of KOH in MeOH, was added dropwise. After stirring at 65°C for 2 h, the resulting suspension was allowed to cool at room temperature and then it was filtered. The filtrate was set aside in dark to evaporate slowly at room temperature and, in a week, crystals of **5** were grown, which were collected. Yield: 0.151 g (36%). Anal. Calcd for C₄₁H₃₉AgN₄OP₂S₂: C, 58.78; H, 4.69; N, 6.69. Found: C, 58.52; H, 4.88; N, 6.82. FTIR (KBr, cm⁻¹): 3273br, 3050w, 1604s, 1503vs, 1479s, 1434vs, 1388vs, 1314s, 1182m, 1094s, 1027s, 998s, 743vs, 693vs, 517vs, 507vs, 485s. UV/Vis (CH₃CN), λ /nm (ϵ): 260 (4.31), 319 (3.39).

2.3 Instrumentation

Elemental analyses were obtained on a PerkinElmer 240B elemental microanalyzer. Infrared spectra were recorded on a Nicolet FT-IR 6700 spectrophotometer as KBr discs in the region of 4000-400 cm⁻¹. The UV-visible (UV-Vis) spectra were obtained on a Hitachi U-2001 dual beam spectrophotometer as solutions (concentrations in the range of 10⁻⁵-10⁻³ M) in CH₂Cl₂, CH₃CN or DMSO. All fluorescence spectra were obtained on a Hitachi F-7000 fluorescence spectrometer. The viscosity experiments were carried out using an ALPHA L

Fungilab rotational viscometer equipped with an 18-mL LCP spindle and the measurements were performed at 100 rpm.

2.4 X-ray crystal structure determinations

Single-crystals of all compounds, suitable for X-ray crystallographic analysis, were mounted on thin glass fibers with the aid of an epoxy resin. X-ray diffraction data were collected on a Bruker Apex II CCD area-detector diffractometer, equipped with a Mo K α ($\lambda = 0.71070 \text{ \AA}$) sealed tube source, at 295 K, using the φ and ω scans technique. The program Apex2 (Bruker AXS, 2006) was used in data collection, cell refinement, and data reduction [15]. Structures were solved and refined with full-matrix least-squares using the program Crystals [16]. Anisotropic displacement parameters were applied to all non-hydrogen atoms, while hydrogen atoms were generated geometrically and refined using a riding model. Details of crystal data and structure refinement parameters are shown on Table 1. Molecular plots were obtained by using the program Mercury [17].

Table 1. Crystal data, data collection and refinement parameters for compounds **1 - 5**

	1	2	3-CH₃OH	4-CH₃CN	5-CH₃CN-CH₃OH
Chemical formula	C ₃₉ H ₃₄ AgClN ₂ P ₂ S ₂	C ₄₄ H ₃₆ AgClN ₂ OP ₂ S	C ₅₈ H ₄₉ AgN ₂ OP ₃ S ₂	C ₅₈ H ₅₁ AgN ₄ P ₃ S ₂	C ₄₁ H ₄₀ AgN ₄ OP ₂ S ₂
Formula weight	800.11	846.12	1054.96	1068.96	838.74
Crystal system	Monoclinic	Triclinic	Triclinic	Triclinic	Triclinic
Space group	<i>P</i> 2 ₁ / <i>c</i>	<i>P</i> -1	<i>P</i> -1	<i>P</i> -1	<i>P</i> -1
Temperature (K)	295	295	295	295	295
Unit cell parameters					
<i>a</i> (Å)	14.4611(11)	11.6739(4)	13.4564(5)	13.5636(6)	13.4227(10)
<i>b</i> (Å)	10.2270(7)	13.6222(5)	13.4668(4)	13.9812(5)	13.6402(10)
<i>c</i> (Å)	25.2849(18)	14.0160(5)	14.5996(5)	14.1258(6)	13.8463(10)
α (°)	90	72.868(2)	78.788(1)	85.831(2)	113.765(3)
β (°)	99.697(1)	82.202(2)	86.062(2)	77.430(2)	110.771(3)
γ (°)	90	70.395(1)	86.000(1)	86.410 (2)	102.632(3)
Volume (Å ³)	3686.0(5)	2004.82(13)	2584.74(15)	2604.61(19)	1966.1(3)
<i>Z</i>	4	2	2	2	2
Radiation type, λ (Å)	Mo <i>K</i> α , 0.71073	Mo <i>K</i> α , 0.71073	Mo <i>K</i> α , 0.71073	Mo <i>K</i> α , 0.71073	Mo <i>K</i> α , 0.71073
Absorption coefficient (mm ⁻¹)	0.85	0.74	0.61	0.60	0.74
Crystal size (mm)	0.25×0.19×0.17	0.33×0.29×0.25	0.37×0.25×0.23	0.21×0.19×0.15	0.28×0.27×0.19
Diffractometer	Bruker Kappa Apex2	Bruker Kappa Apex2	Bruker Kappa Apex2	Bruker Kappa Apex2	Bruker Kappa Apex2
Absorption correction	Numerical	Numerical	Numerical		
<i>T</i> _{min} , <i>T</i> _{max}	0.85, 0.87	0.81, 0.83	0.86, 0.87	0.89, 0.91	0.82, 0.87
Number of measured, independent and observed [<i>I</i> > 2.0 σ (<i>I</i>)] reflections	43700, 10435, 8471	26934, 8255, 7048	85296, 11594, 8908	42919, 10798, 8307	38032, 11421, 7659
<i>R</i> _{int}	0.023	0.012	0.037	0.013	0.107
(<i>sin</i> θ / λ) _{max} (Å ⁻¹)	0.697	0.631	0.647	0.630	0.711
<i>R</i> [<i>F</i> ² > 2 σ (<i>F</i> ²)], <i>wR</i> (<i>F</i> ²), <i>S</i>	0.036, 0.063, 1.00	0.020, 0.028, 1.00	0.041, 0.065, 1.00	0.031, 0.060, 1.00	0.064, 0.103, 1.00
No. of reflections	8418	7048	8908	8307	7659
No. of parameters	424	469	602	611	460
$\Delta\rho_{\max}$, $\Delta\rho_{\min}$ (e Å ⁻³)	0.56, -0.53	0.38, -0.23	1.26, -0.98	0.59, -0.48	1.51, -0.96

2.5 Study of the interaction of the compounds with calf-thymus (CT) DNA

In order to study *in vitro* the interaction of complexes **1-5** with CT DNA, the compounds were initially dissolved (1 mM) in DMSO or, for complex **3**, in CH₃CN. Mixing of such solutions with the aqueous buffer DNA-containing solutions used in the studies never exceeded 5% DMSO (v/v) in the final solution, which was needed due to low aqueous solubility of most compounds. Control experiments with DMSO or CH₃CN were performed and no changes in the spectra of CT DNA were observed.

The investigation of the possible DNA-binding mode of complexes **1-5** and the calculation of the corresponding DNA-binding constants (K_b) were carried out by UV-vis spectroscopy. The UV-vis spectra of CT DNA were recorded for a constant DNA concentration ($1.2-1.6 \times 10^{-4}$ M) in the presence of each compound at diverse [complex]/[DNA] mixing ratios (= r). The DNA-binding constant (K_b in M^{-1}) is obtained by monitoring the changes in the absorbance at the corresponding λ_{max} for a constant concentration ($2-5 \times 10^{-5}$ M) with increasing concentrations of CT DNA and it is given by the ratio of slope to the y intercept in plots $[DNA]/(A - \epsilon_f)$ versus $[DNA]$ (Fig. S2), according to the Wolfe-Shimer equation [18]:

$$\frac{[DNA]}{(\epsilon_A - \epsilon_f)} = \frac{[DNA]}{(\epsilon_b - \epsilon_f)} + \frac{1}{K_b(\epsilon_b - \epsilon_f)} \quad (\text{eq. 1})$$

where $[DNA]$ is the concentration of DNA in base pairs, $A = A_{obsd}/[compound]$, ϵ_f = the extinction coefficient for the free compound and ϵ_b = the extinction coefficient for the compound in the fully bound form.

The viscosity of DNA ($[DNA] = 0.1$ mM) in buffer solution (150 mM NaCl and 15 mM trisodium citrate at pH 7.0) was measured in the presence of increasing amounts of temperature and the obtained data are presented as $(\eta/\eta_0)^{1/3}$ versus r , where η is the viscosity of DNA in the presence of the compound, and η_0 is the viscosity of neat DNA in buffer solution.

Fluorescence emission spectroscopy was used in order to examine whether each complex may compete with EB for the DNA-intercalating sites by displacing it from its DNA-EB

conjugate. The DNA-EB conjugate was prepared by adding 20 μM EB and 26 μM CT DNA in buffer solution (150 mM NaCl and 15 mM trisodium citrate at pH 7.0). The possible intercalating effect of the complexes was studied by a stepwise addition of a certain amount of a compound's solution into a EB-DNA solution. The resultant changes were monitored by recording the variation of fluorescence emission spectra with excitation wavelength at 540 nm. Complexes **1-5** do not show any appreciable fluorescence emission bands at room temperature in solution or in the presence of DNA or EB under the same experimental conditions ($\lambda_{\text{excitation}} = 540 \text{ nm}$); therefore, the observed quenching may be attributed to the displacement of EB from its EB-DNA conjugate. The Stern-Volmer constant (K_{sv} , in M^{-1}) is used to evaluate the quenching efficiency for each compound according to the Stern-Volmer equation (eq. 2) [19,20]:

$$\frac{I_0}{I} = 1 + k_q \tau_0 [Q] = 1 + K_{\text{sv}} [Q] \quad (\text{eq. 2})$$

where I_0 and I are the emission intensities of the EB-DNA solution in the absence and the presence of the quencher, respectively, $[Q]$ is the concentration of the quencher (i.e. complexes **1-5**), τ_0 = the average lifetime of the emitting system without the quencher and k_q = the quenching constant. K_{sv} is calculated from the Stern-Volmer plots (Fig. S8) by the slope of the diagram I_0/I versus $[Q]$. Taking $\tau_0 = 23 \text{ ns}$ as the fluorescence lifetime of the EB-DNA system [21], the quenching constants (k_q , in $\text{M}^{-1}\text{s}^{-1}$) of the compounds can be determined according to eq. 3:

$$K_{\text{sv}} = k_q \tau_0 \quad (\text{eq. 3})$$

2.6 Antimicrobial studies

The antibacterial activities of 1-5 against four bacterial species [*Escherichia coli* (*E. coli*), *Bacillus subtilis* (*B. subtilis*), *Bacillus cereus* (*B. cereus*) and *Staphylococcus aureus* (*S. aureus*)] were estimated by the minimum inhibitory concentration (MIC) method as described earlier [22]. The cultivation media used for antimicrobial activity tests were: (i) the

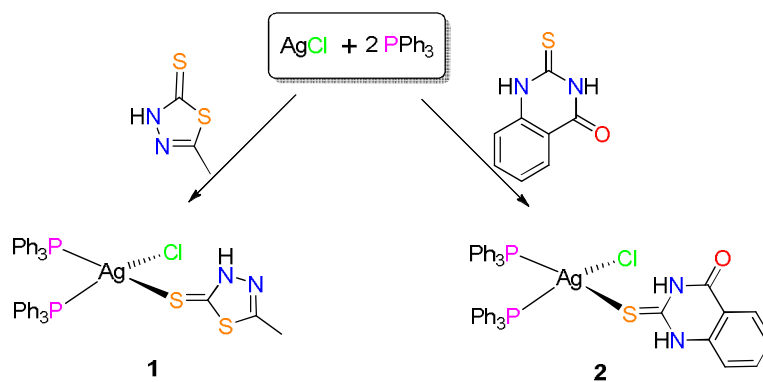
Luria-Bertani broth containing 1% (w/v) tryptone, 0.5% (w/v) NaCl and 0.5% (w/v) yeast extract and (ii) the minimal medium salts broth containing 1.5% (w/v) glucose, 0.5% (w/v) NH₄Cl, 0.5% (w/v) K₂HPO₄, 0.1% (w/v) NaCl, 0.01% (w/v) MgSO₄·7H₂O and 0.1% (w/v) yeast extract. The pH of the media was adjusted to 7.0.

3. RESULTS AND DISCUSSION

3.1 Synthesis and crystal structures

Reactions of silver(I) salts with heterocyclic thioamides Ar^{NH}S or thioamides Ar^NS, in the presence of triarylphosphines PR₃, depending on the nature of thioamide and phosphine, as well as the reactions conditions. e.g. stoichiometric ratios, can result in compounds with a variety of structural motifs [1,2,8,9]. Aiming to the synthesis of mononuclear compounds of silver(I) having a specific mixed set of sulfur- and phosphorus-donor atom ligands, we attempted reactions of various silver(I) salts with three heterocyclic thioamides that differ in their stereochemical and electronic properties, i.e. mtdztH, amtdztH, and mqzH (Scheme 1), either in their neutral or deprotonated forms, in the presence of PPh₃, using different stoichiometric reactant ratios.

In particular, the reactions of AgCl with the heterocyclic thioamides mtdztH and mqzH, in the presence of two equivalents of PPh₃, in a MeCN/MeOH mixture, afforded mononuclear mixed-ligand complexes with the general formula [AgCl(PPh₃)₂(κ-S-Ar^{NH}S)], Ar^{NH}S = mtdztH (**1**) and mqztH (**2**), in which the thioamide ligands act in an S-terminal bonding mode (Scheme 2).



Scheme 2. Synthesis of compounds **1** and **2**

Single-crystals of the two compounds, suitable for X-ray crystallographic analysis, were obtained by slow evaporation of their corresponding reaction mixtures. Views of the molecular structures of compounds **1** and **2** are shown in Fig. 1 and 2, while selected bond length and angle parameters are summarized in Table 1. Both are mononuclear compounds having the silver atoms in tetrahedral coordination environments which are completed by the exocyclic sulfur atoms of a thioamide ligand acting in an S-terminal bonding mode, the phosphorous atoms of two PPh₃ ligands, and a halide atom. Bond angles and distances around the central metal atom (Table 1) reveal distortions from the ideal tetrahedral geometry (for example, P1–Ag1–P2 = 126.24(2)° and Cl1–Ag1–S1 = 96.19(2)°, for compound **1**). The Ag–P and Ag–Cl bond lengths do not differ significantly between the two complexes and they fall in ranges that are normally found for analogous mononuclear silver(I) compounds. The Ag–S bond lengths are slightly different, i.e. 2.7976(7) and 2.7098(4) Å for **1** and **2**, respectively, but they are close to the values found in analogous mononuclear silver(I) complexes containing an S-bound neutral thioamide ligand. Furthermore, both compounds are stabilized by intramolecular hydrogen-bonding interactions developed between the coordinated chlorine atom and the nitrogen atom of the heterocyclic ring of the corresponding thioamide ligand, as it revealed by the relative orientations of two relevant ligands and the short Cl···N distances (at 3.10 and 3.08 Å, for compounds **1** and **2**, respectively).

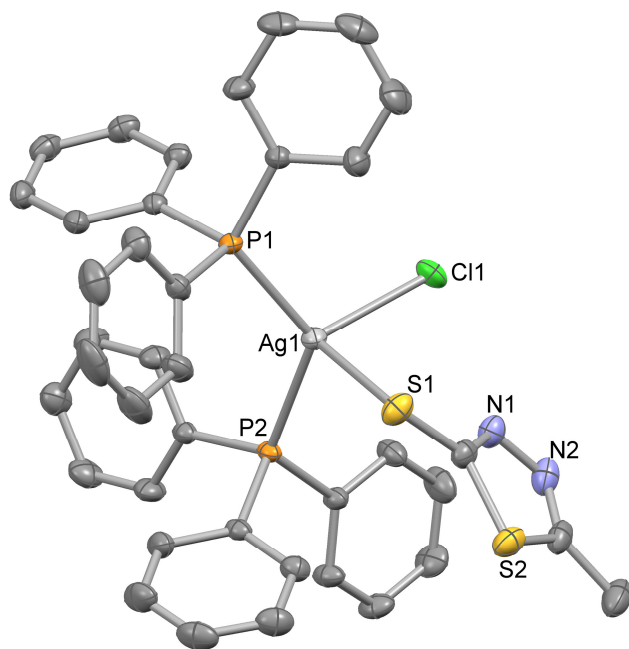


Fig. 1. ORTEP diagram of the molecular structure of compound 1 with displacement ellipsoids drawn at the 35% probability level. All hydrogen atoms have been omitted for clarity.

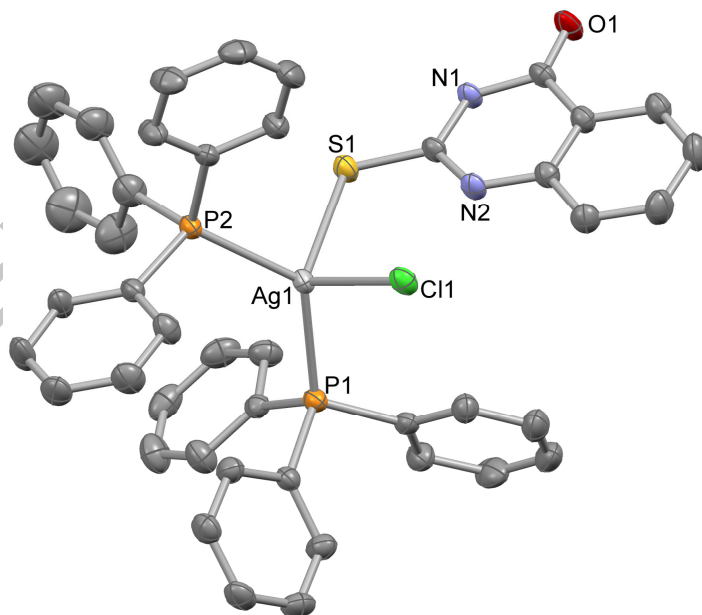
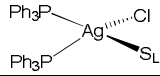


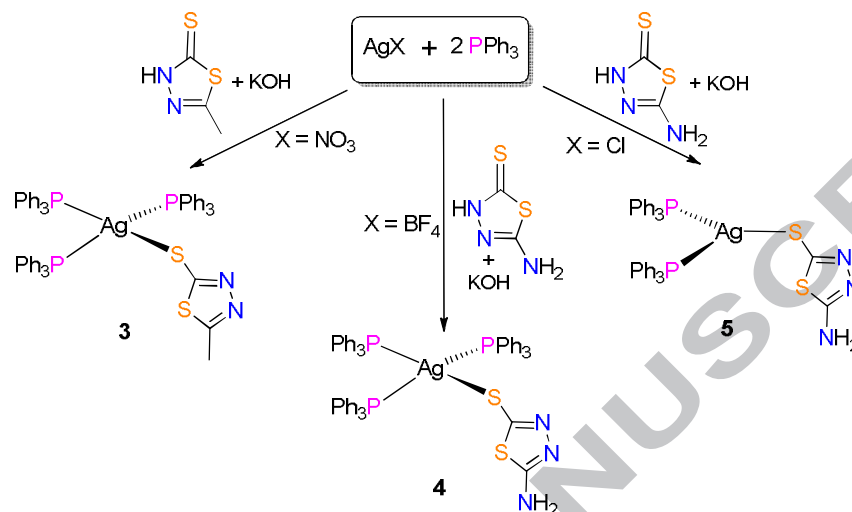
Fig. 2. ORTEP diagram of the molecular structure of compound 2 with displacement ellipsoids drawn at the 35% probability level. All hydrogen atoms have been omitted for clarity.

Table 2. Selected bond lengths (Å) and angles (°) for compounds **1** and **2**.


	1 $S_L = \text{mtdztH}$	2 $S_L = \text{mqzH}$
bond distances		
Ag1–Cl1	2.5706(6)	2.6142(4)
Ag1–P1	2.4618(5)	2.4551(4)
Ag1–P2	2.4875(5)	2.4597(4)
Ag1–S1	2.7976(7)	2.7098(4)
bond angles		
Cl1–Ag1–P1	112.20(2)	105.53(1)
Cl1–Ag1–P2	110.32(2)	108.65(1)
P1–Ag1–P2	126.24(2)	126.70(1)
Cl1–Ag1–S1	96.19(2)	102.34(1)
P1–Ag1–S1	103.74(2)	112.84(1)
P2–Ag1–S1	102.77(2)	98.32(1)

The reactions of the silver(I) salts AgNO_3 and AgBF_4 with the heterocyclic thioamidates mtdzt and amtdzt, respectively (which were obtained upon treatment of the corresponding neutral thioamides mtdztH and amtdztH with equivalent amounts of KOH in MeOH), in the presence of a two-fold excess of PPh_3 , in MeCN, resulted in the formation of a different class of mononuclear silver(I) compounds with the general formula $[\text{Ag}(\kappa\text{-S-Ar}^{\text{N}}\text{S})(\text{PPh}_3)_3]$, $\text{Ar}^{\text{NH}}\text{S} = \text{mtdzt}$ (**3**) and amtdzt (**4**), as shown in Scheme 3. The formulas of the two compounds are not in agreement with the corresponding reaction stoichiometries, since the final product contains three PPh_3 units coordinated to the central metal ion. However, it has not been possible to identify any other product from the corresponding reaction mixtures. In contrast, the analogous reaction of AgCl with the thioamidate salt of amtdztH with two equivalents of PPh_3 , under identical experimental conditions, resulted in the synthesis of the expected

mononuclear mixed-ligand complex $[\text{Ag}(\kappa\text{-S-amtdzt})(\text{PPh}_3)_2]$ (**5**) (Scheme 3). In all cases, the thioamidate ligands act in an S-terminal bonding mode.



Scheme 3. Synthesis of compounds **3**, **4**, and **5**

As shown in Fig. 3 and 4, compounds **3** and **4** are mononuclear complexes with tetrahedrally coordinated silver atoms, whose coordination sphere are completed by the phosphorus atoms of three PPh_3 molecules, and the exocyclic sulfur atom of a thioamidate ligand (mdtzt and amtdzt, respectively). In contrast, compound **5** exhibits a trigonal planar geometry around the metal center having coordinated two PPh_3 molecules and an S-bound amtdzt ligand (Fig. 5). All compounds exhibit slight distortions from their corresponding ideal coordination geometries (see for example in Table 2: $\text{P1-Ag1-P2} = 113.84(3)^\circ$, $114.43(2)^\circ$, $120.61(4)^\circ$, for compounds **3**, **4** and **5**, respectively). In case of the tetrahedrally coordinated compounds **3** and **4**, the Ag–P bond lengths are found to fall in the range of 2.52–2.64 Å, while in the trigonal planar compound **5** these are shorter at 2.4701(11) and 2.4881(11) Å. The Ag–S bond lengths are found to be similar among compounds **3**, **4**, and **5**, i.e. 2.5845(9), 2.5571(7), and 2.5238(12), respectively. Noticeably, these are shorter than the

corresponding Ag–S distances observed in the mononuclear silver(I) complexes **1** and **2**, a fact that can be ascribed to the anionic nature of the S-bound thioamidate ligands they contain, compared to the neutral mtdztH and mqzH ligands of compounds **1** and **2** discussed above.

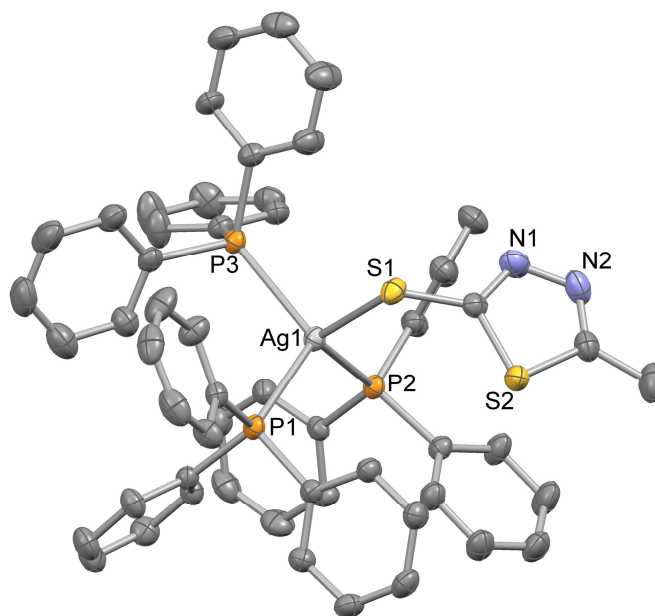


Fig. 3. ORTEP diagram of the molecular structure of compound **3** with displacement ellipsoids drawn at the 35% probability level. All hydrogen atoms have been omitted for clarity.

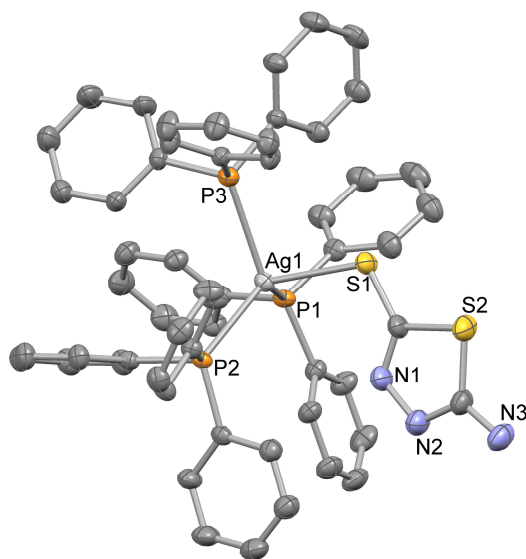


Fig. 4. ORTEP diagram of the molecular structure of compound **4** with displacement ellipsoids drawn at the 35% probability level. All hydrogen atoms have been omitted for clarity.

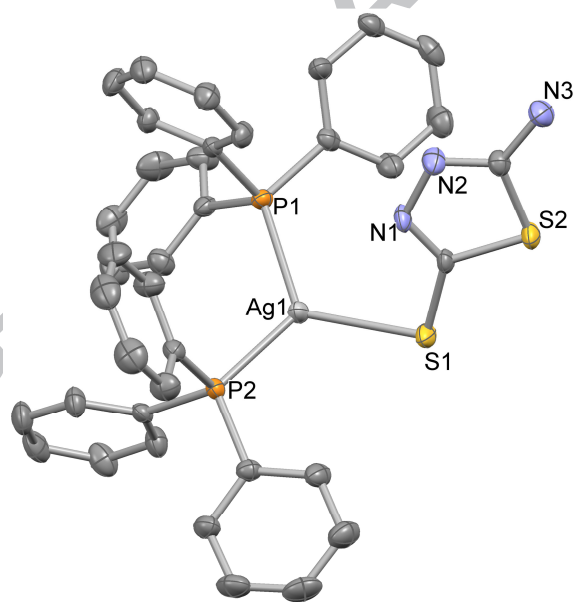
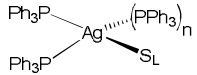


Fig. 5. ORTEP diagram of the molecular structure of compound **5** with displacement ellipsoids drawn at the 35% probability level. All hydrogen atoms have been omitted for clarity.

Table 3. Selected bond lengths (Å) and angles (°) for compounds **3**, **4**, and **5**.


	3 L = mtdzt, n = 1	4 L = atdzt, n = 1	5 L = atdzt, n = 0
bond distances			
Ag1–P1	2.6019(8)	2.5854(7)	2.4881(11)
Ag1–P2	2.5219(8)	2.5537(6)	2.4701(11)
Ag1–P3	2.6400(8)	2.6405(7)	
Ag1–S1	2.5845(9)	2.5571(7)	2.5238(12)
bond angles			
P1–Ag1–P2	113.84(3)	114.43(2)	120.61(4)
P1–Ag1–P3	112.83(3)	114.48(2)	
P2–Ag1–P3	110.08(3)	111.74(2)	
P1–Ag1–S1	97.75(3)	101.54(3)	116.65(4)
P2–Ag1–S1	114.67(3)	119.50(2)	121.80(4)
P3–Ag1–S1	107.06(3)	93.25(2)	

From the aforementioned results, it is clear that reactions of silver(I) halide salts, such as AgCl, with heterocyclic thioamides $\text{Ar}^{\text{NH}}\text{S}$, in the presence of two equivalents of PPh_3 , result in the synthesis of mononuclear silver(I) complexes $[\text{AgCl}(\text{PPh}_3)_2(\kappa\text{-S-Ar}^{\text{NH}}\text{S})]$, as expected from the reaction stoichiometry. In contrast, the analogous reactions of silver(I) salts with heterocyclic thioamidates $\text{Ar}^{\text{N}}\text{S}$ can lead to the synthesis of different compounds whose identity depends on the type of the silver(I) starting materials used in each case. In particular, the utilization of AgCl led to the synthesis of a mononuclear complex with trigonal coordination geometry and two molecules of PPh_3 coordinated to the Ag(I) ion, i.e. $[\text{Ag}(\kappa\text{-S-Ar}^{\text{N}}\text{S})(\text{PPh}_3)_2]$. However, the use of silver(I) salts which contain weakly- or non-coordinating anions, such as BF_4^- or NO_3^- , give rise to complexes $[\text{Ag}(\kappa\text{-S-Ar}^{\text{N}}\text{S})(\text{PPh}_3)_3]$, which contain a tetrahedrally coordinated metal ion having three molecules of PPh_3 in its coordination sphere.

Corroborating evidence for the identity of the five new compounds in bulk form, as well as verification of the coordination mode of both triphenylphosphine and the respective thioamide ligands, has been obtained by Infra-red spectroscopy. The infrared spectra of compounds **1–5**, recorded in the range $4000\text{--}200\text{ cm}^{-1}$ are dominated by characteristic bands due to the presence of the respective heterocyclic thioamide ligand. For example, the intense bands at 1550 cm^{-1} and 1268 cm^{-1} in the spectrum of free mtdztH, attributed to the C–N stretching vibration of the thioamide moiety, appear in the spectrum of compound **3** shifted to 1579 cm^{-1} and 1307 cm^{-1} respectively, indicating an exclusive S-coordination of the ligand. Likewise, the band at 1095 cm^{-1} assigned to the C=S stretching [23], is shifted to lower energies (1087 cm^{-1}) due to S-coordination. Analogous conclusions are drawn from the IR spectra of the other compounds. Analogous conclusions are drawn from the IR spectra of the other compounds.

3.3 Interaction of the compounds with CT DNA

The mode of interaction between metal complexes and double-stranded DNA depends on the structure of the complexes and the nature of the ligands including covalent interaction, non-covalent interaction and cleavage of the DNA-helix [24]. Covalent interaction between metal complexes and double-stranded DNA takes place upon the displacement of a labile ligand of the complex by DNA-base. Non-covalent interactions are of three different types, i.e. intercalation *via* • stacking interactions between the planar aromatic rings of the complex and DNA-bases, electrostatic interactions when Coulomb forces appear between a cationic complex and the negative phosphate groups of DNA, and groove-binding in the presence of hydrophobic or hydrogen bonding or van der Waals forces. Herein, in order to investigate the interaction of the compounds with CT DNA, UV-vis spectroscopy, DNA-viscosity measurements and competitive studies with EB (by fluorescence emission spectroscopy) have been employed.

UV-vis spectroscopy was used in order to examine the DNA-binding mode and to calculate the DNA-binding strength. Any changes observed in the DNA UV-band or the intraligand transition bands of the complexes may reveal the existence of any interaction and its possible mode. The UV-vis spectra of a CT DNA solution in the presence of mtdztH and complex **5** at increasing r values are shown representatively in Fig. 6. The band at $\lambda_{\text{max}} = 258$ nm exhibits a slight hypochromism accompanied by a red-shift up to 261 nm, suggesting the existence of interaction between CT DNA and the compounds. Such interaction leads to the formation of a new compound-DNA conjugate [25] resulting in stabilization of the CT DNA double-helix [26]. Similar changes in the UV spectrum of a CT DNA solution are also observed in the presence of the other compounds.

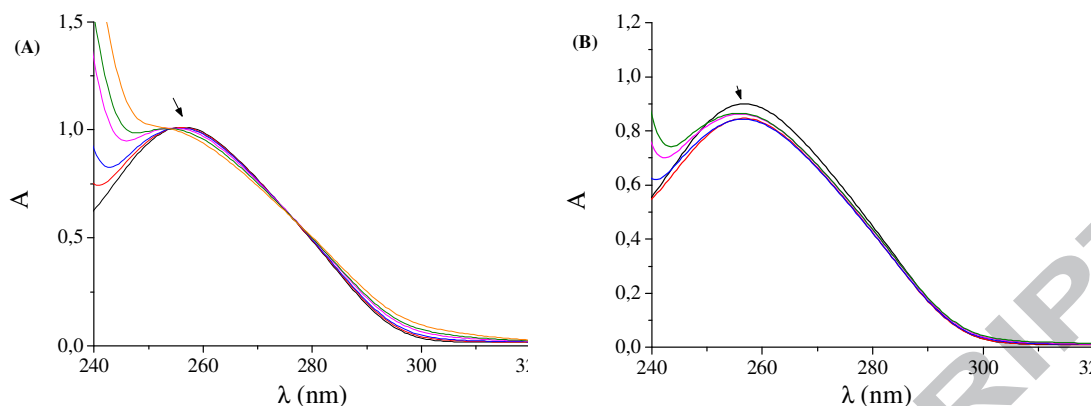


Fig. 6. (A) UV-vis spectra of CT DNA (0.150 mM) in buffer solution (150 mM NaCl and 15 mM trisodium citrate at pH 7.0) in the absence or presence of mtdztH. The arrows show the changes upon increasing amounts of the compound. (B) UV-vis spectra of CT DNA (0.136 mM) in buffer solution (150 mM NaCl and 15 mM trisodium citrate at pH 7.0) in the absence or presence of complex **5**. The arrows show the changes upon increasing amounts of the complex.

In the UV-vis spectra of the thioamides (Fig. 7(A) and Fig. S1(A) and (B)), the UV-band located in the range 293-320 nm presents in the presence of increasing amounts of CT DNA a hypochromism up to 29%. In the UV spectra of complexes **1-5**, the intraligand band located in the range 253-283 nm presents a moderate hyperchromism (Fig. 7(B) and (C), and Fig. S1(C)-(E)), while the second intraligand band observed for complexes **1, 4** and **5** in the range 310-320 nm exhibits a significant hypochromism followed by its disappearance. The significant percentage of hypochromism observed for complexes **1, 4** and **5** may be attributed to → stacking interactions between the complexes and DNA-bases [27] and might be consistent of an intercalative binding mode leading to a stabilization of the DNA helix [26]. Nevertheless, safe conclusions cannot be merely derived for all compounds from UV-vis spectroscopic titrations studies and DNA-viscosity measurements were performed in order to clarify the DNA-binding mode of the compounds.

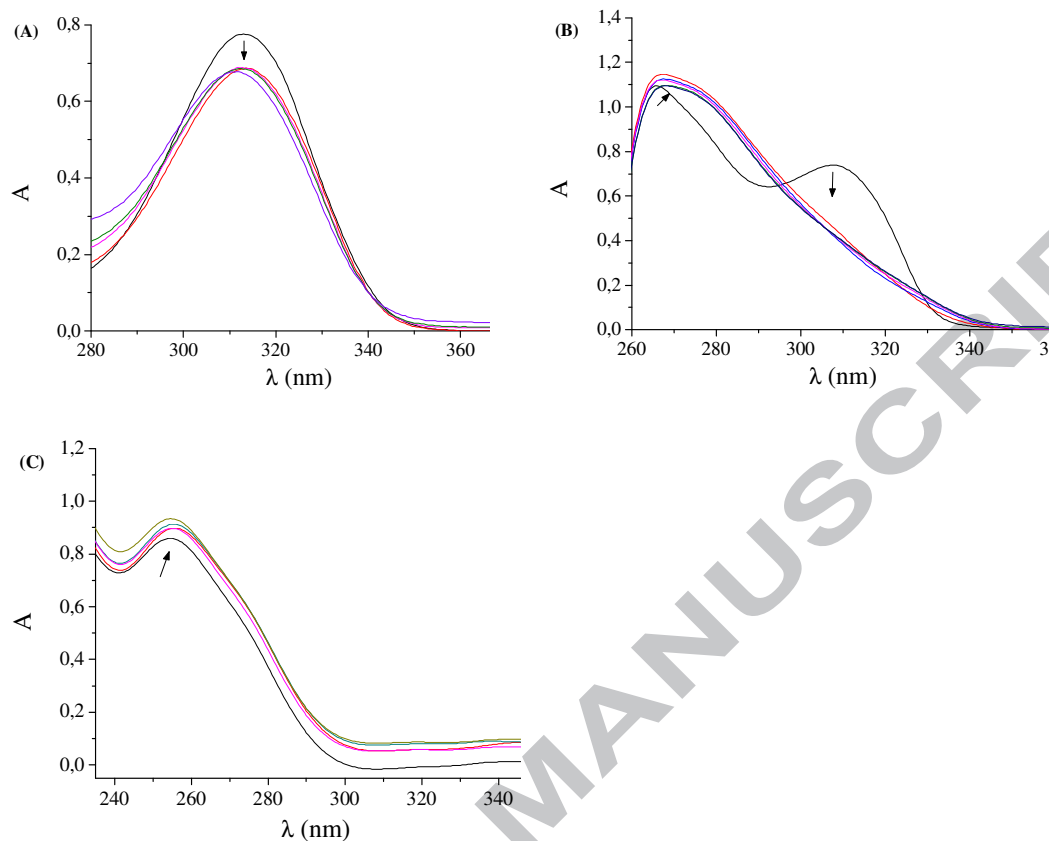


Fig. 7. UV-vis spectra of solutions of (A) mtdztH (5×10^{-5} M) in DMSO, (B) complex **1** (5×10^{-5} M) in DMSO and (C) complex **3** (2.5×10^{-5} M) in CH_3CN , in the presence of increasing amounts of CT DNA ($r' = [\text{DNA}]/[\text{compound}] = 0-0.8$). The arrows show the changes upon increasing amounts of CT DNA.

The DNA-binding constants (K_b) of the compounds (Table 4) were calculated by the Wolfe-Shimer equation [27] (eq. 1) and the corresponding plots $[\text{DNA}]/(\lambda_{\text{max}} - \lambda_{\text{max}}^0)$ versus $[\text{DNA}]$ (Fig. S2). The K_b constants of the compounds (Table 4) are significantly high and suggest strong binding of the complexes to CT DNA with complex **4** ($=6.35(\pm 0.05) \times 10^7 \text{ M}^{-1}$) showing the highest affinity for CT DNA among complexes **1-5**. In average, the K_b constants are similar or higher than that of the classical intercalator EB ($= 1.23 \times 10^5 \text{ M}^{-1}$) as calculated by Dimitrakopoulou et al [28].

Table 4. UV-vis spectral features of the interaction of complexes **1-5** with CT DNA: UV-band (λ , in nm) (percentage of hyper-/hypo-chromism ($\Delta A/A_0$, in %), blue-/red-shift of λ_{max} ($\Delta\lambda$, in nm)) and DNA-binding constants (K_b , in M^{-1}).

Compound	λ (nm) ($\Delta A/A_0$ % ($\% ^a$), $\Delta\lambda$ (nm) b)	K_b (M^{-1})
mtdzH	313 (-12, 0)	$7.34(\pm 0.02)\times 10^7$
mqztH	293 (-29, +5)	$1.24(\pm 0.19)\times 10^6$
atdzH	320 (-22, -10)	$1.01(\pm 0.24)\times 10^6$
[AgCl(PPh ₃) ₂ (mtdzH)] (1)	266 (+11, 5), 310 (-48, elm ^c)	$3.63(\pm 0.11)\times 10^6$
[AgCl(PPh ₃) ₂ (mqztH)] (2)	283 (+3.6, 0)	$1.27(\pm 0.01)\times 10^7$
[Ag(PPh ₃) ₃ (mtdzH)] (3)	253 (+9, 0)	$1.62(\pm 0.10)\times 10^6$
[Ag(PPh ₃) ₃ (atdzH)] (4)	267 (+4.5, +3), 320 (-60, elm)	$6.35(\pm 0.05)\times 10^7$
[Ag(PPh ₃) ₂ (atdzH)] (5)	272 (+15, 0), 315 (-20, elm)	$1.78(\pm 0.10)\times 10^4$

^a “+” denotes hyperchromism, “-” denotes hypochromism

^b “+” denotes red-shift, “-” denotes blue-shift

^c “elm” = eliminated

In order to further investigate the interaction of the compounds with CT DNA, the changes of the DNA-viscosity induced by the presence of the complexes in increasing amounts were also monitored. It is known that the relative DNA-viscosity (η/η_0) is related to the relative DNA-length (L/L_0) via the equation $L/L_0 = (\eta/\eta_0)^{1/3}$ [28]. Therefore, any changes of the relative DNA-viscosity occurring in the presence of a DNA-binder may reveal the changes of relative DNA-length and subsequently the possible mode of DNA-interaction. In the case of intercalation, the DNA-viscosity presents a significant increase, while in the case of non-classical intercalation (including groove-binding or electrostatic interaction), the DNA-viscosity may decrease slightly or remain unchanged [29].

The changes of the viscosity of a CT DNA solution (0.1 mM) were in the presence of increasing amounts of complexes **1-5** (up to the value of $r = 0.35$). For all complexes, the DNA-viscosity has shown a considerable increase upon their addition (Fig. 8). This increase

may be attributed to intercalation of the complexes in-between DNA-bases, since in the case of intercalation, the separation distance of the DNA bases will increase in order to accommodate the intercalating compounds and subsequently the DNA-viscosity is increased [29]. The existing conclusion of intercalation may clarify and enforce the preliminary conclusions derived from the UV-vis spectroscopic studies.

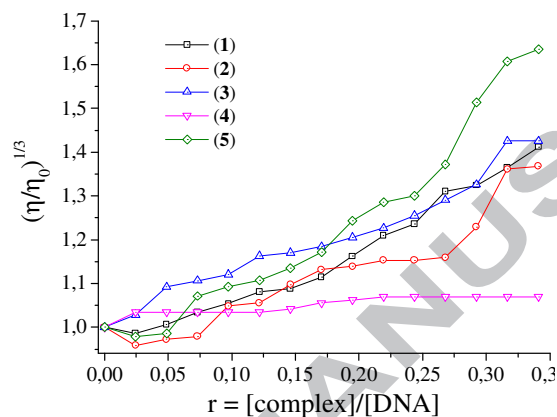


Fig. 8. Relative viscosity $(\eta/\eta_0)^{1/3}$ of CT DNA (0.1 mM) in buffer solution (150 mM NaCl and 15 mM trisodium citrate at pH 7.0) in the presence of complexes **1-5** at increasing amounts *versus* $r = [\text{complex}]/[\text{DNA}]$.

Ethidium bromide is a DNA-intercalator. The intercalation takes place *via* the planar EB-phenanthridine ring which inserts in-between the DNA-base pairs resulting in the appearance of an intense fluorescence emission band at 592 nm upon excitation of the EB-DNA solution at 540 nm. When a compound able to intercalate equally or more strongly than EB is added into the EB-DNA solution, a remarkable quenching of the EB-DNA fluorescence emission band may appear [19,30]. Therefore, the emission spectra of pre-treated EB-CT DNA ($[\text{EB}] = 20 \mu\text{M}$, $[\text{DNA}] = 26 \mu\text{M}$) in the absence and presence of each complex were recorded in the presence of increasing amounts of the compounds up to the value of $r = 0.30$ (representatively shown for complex **3** in Fig. 9(A)).

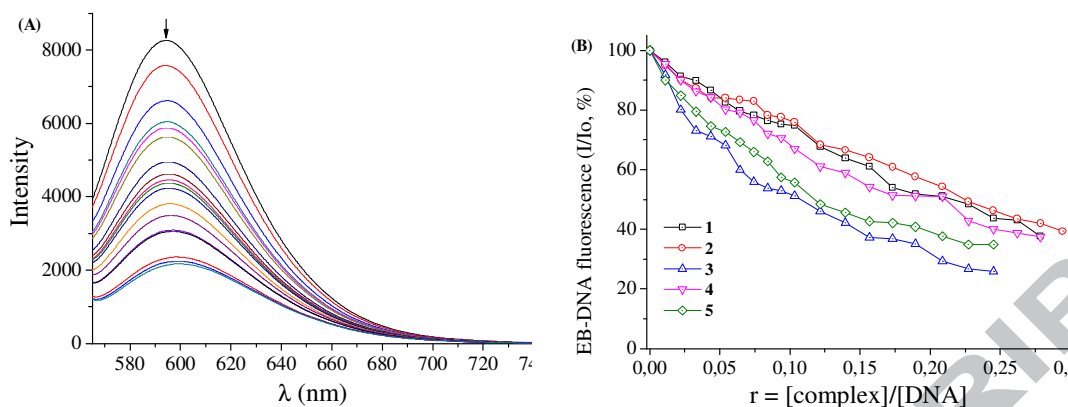


Fig. 9. (A) Fluorescence emission spectra ($\lambda_{exc} = 540$ nm) for EB-DNA ($[EB] = 20 \mu\text{M}$, $[DNA] = 26 \mu\text{M}$) in buffer solution in the absence and presence of increasing amounts of complex **3** (up to the value of $r = 0.28$). The arrow shows the changes of intensity upon increasing amounts of **3**. (B) Plot of EB-DNA relative fluorescence intensity ($I/I_0\%$) at $\lambda_{em} = 592$ nm versus r ($r = [\text{complex}]/[\text{DNA}]$) in buffer solution (150 mM NaCl and 15 mM trisodium citrate at pH 7.0) in the presence of complexes **1-5** (quenching up to 37.6% of the initial EB-DNA fluorescence for **1**, 39.3% for **2**, 25.8% for **3**, 37.5% for **4** and 34.9% for **5**).

The addition of the complexes resulted in a significant quenching (Fig. 9(B)) of the emission band of the EB-DNA system at 592 nm up to 74.2% of the initial EB-DNA fluorescence (Table 5). Since the complexes do not exhibit any fluorescence emission band at room temperature in solution or in the presence of CT DNA under the same experimental conditions (i.e. $\lambda_{excitation} = 540$ nm), the observed quenching of the EB-DNA emission band may be attributed to the competition of the complexes with EB for the DNA-intercalation sites.

Table 5. Fluorescence features of the EB-displacement studies of the ligands and complexes **1-5**: percentage of EB-DNA fluorescence emission quenching ($\Delta I/I_0$, in %), Stern-Volmer (K_{sv} , in M^{-1}) and quenching constants (k_q , in $M^{-1}s^{-1}$).

Compound	$\Delta I/I_0$ %	K_{sv} (M^{-1})	k_q ($M^{-1}s^{-1}$)
[AgCl(PPh ₃) ₂ (mtdtH)] (1)	62.4	$1.14(\pm 0.03) \times 10^5$	$4.96(\pm 0.13) \times 10^{12}$
[AgCl(PPh ₃) ₂ (mqztH)] (2)	60.1	$1.72(\pm 0.06) \times 10^5$	$7.46(\pm 0.24) \times 10^{12}$
[Ag(PPh ₃) ₃ (mtdzt)] (3)	74.2	$5.32(\pm 0.15) \times 10^5$	$2.31(\pm 0.07) \times 10^{13}$
[Ag(PPh ₃) ₃ (atdzt)] (4)	62.5	$1.40(\pm 0.03) \times 10^5$	$6.10(\pm 0.15) \times 10^{12}$
[Ag(PPh ₃) ₂ (atdzt)] (5)	65.1	$3.71(\pm 0.09) \times 10^5$	$1.61(\pm 0.04) \times 10^{13}$
mtdztH	54.9	$1.16(\pm 0.02) \times 10^5$	$5.03(\pm 0.10) \times 10^{12}$
mqztH	63.2	$3.26(\pm 0.10) \times 10^5$	$1.42(\pm 0.05) \times 10^{13}$
atdztH	62.5	$1.41(\pm 0.07) \times 10^5$	$6.13(\pm 0.03) \times 10^{12}$

The linear Stern-Volmer equation (eq. 2) and the corresponding Stern-Volmer plots (Fig. S2, $R = 0.99$) may confirm that the observed quenching of the EB-DNA fluorescence may be attributed to the competition of the complexes with EB. Subsequently, it may be proposed that the complexes may displace EB from its conjugate with DNA. Therefore, the existence of intercalation of the complexes in-between CT DNA may be indirectly confirmed [20]. The values of the K_{sv} constants of the complexes (Table 5) are high enough and confirm their ability to bind to DNA with complex **3** bearing the highest K_{sv} value ($=5.32(\pm 0.15) \times 10^5 M^{-1}$) among the complexes. The EB-DNA quenching constants (k_q) for the compounds were calculated according to eq. 3, since the EB-DNA system fluorescence lifetime of has the value $\tau_0 = 23$ ns [21]. The k_q constants (Table 5) are much higher than the value of $10^{10} M^{-1}s^{-1}$ and may suggest that the quenching of the EB-DNA fluorescence induced by the complexes takes place *via* a static mechanism [19] leading to the formation of a new conjugate, i.e. complex-DNA.

3.4 Antibacterial activity

The antibacterial activity of the silver (I) complexes **1-5** (average of three measurements) as well as of AgCl and the free ligands PPh₃, mtdztH, atdzH, ptztH was estimated by monitoring the growth of certain Gram-positive (*Bacillus subtilis*, *Bacillus cereus*, *Staphylococcus aureus*) and Gram-negative (*Escherichia coli*) bacterial strains in the presence of various concentrations of these complexes and ligands ranging from 0 to 100 µg·mL⁻¹. The minimum half inhibitory concentration (IC₅₀) values obtained for each strain and each compound are presented in Table 6.

Table 6. Antimicrobial activities of the free ligands PPh₃, mtdztH, atdzH and mqztH and the complexes (**1-5**) evaluated by the half-minimal inhibitory concentration (IC₅₀) (µg·mL⁻¹ and µ in parentheses).

Compound	<i>S. aureus</i>	<i>B. cereus</i>	<i>B. Subtilis</i>
PPh ₃	51 (194)	70 (267)	>100 (>380)
mtzdtH	21 (159)	32 (242)	53 (401)
atdzH	40 (300)	40 (300)	60 (450)
mqztH	55 (308)	55 (308)	50 (280)
[AgCl(PPh ₃) ₂ (mtzdtH)] (1)	16 (20)	21 (26)	81 (101)
[AgCl(PPh ₃) ₂ (mqztH)] (2)	16 (19)	35 (41)	35 (41)
[Ag(PPh ₃) ₃ (mtzdt)] (3)	17 (16)	20 (19)	12.5(12)
[Ag(PPh ₃) ₃ (atdz)] (4)	18 (21)	25 (30)	32 (38)
[Ag(PPh ₃) ₂ (atdz)] (5)	9 (8)	10 (9)	20 (18)

As it can be seen from the data tabulated in Table 6, the antibacterial activity of the compounds under study is clearly higher when compared to that of the starting materials. Note that no activity was found for AgCl against any of the bacteria investigated. In addition, only a negligible activity against *E. coli* could be determined for all the compounds. This latter finding appears somewhat unexpected and contradicts our previous results on similar

silver(I) compounds. Considering the activity of compounds **1-5** against each of the Gram-positive strains, the IC_{50} values are not significantly different from each other and do not follow a particular order, therefore not sufficient to suggest any relation between effectiveness and any structural characteristics of the complexes. The only fact from which one could suggest a relation between effectiveness and structural characteristics of the complexes results from the comparison of the activities of compounds **4** and **5**. In particular, the trigonal planar compound **5** is twice as active as the tetrahedral one (compound **4**) against all bacteria strains, though these two compounds contain the same thioamide ligand. Nevertheless, even this cannot be regarded as a meaningful conclusion, especially due to the fact that it is not in line with the outcome of our previous investigations on related compounds.

4. CONCLUDING REMARKS

Herein we report the synthesis and crystal structures of five neutral silver(I) complexes, exhibiting tetrahedral or trigonal planar coordination geometries around the metal center, and bearing as ligands combinations of different heterocyclic thioamides (or thioamidates) and a varying number of PPh_3 molecules. Significant *in vitro* antibacterial activity has been found for all the complexes against certain Gram-positive (*Bacillus subtilis*, *Bacillus cereus*, *Staphylococcus aureus*) bacterial strains. Regarding the relation between activity and structural characteristics, for complexes bearing the same thioamide ligand, the effectiveness seem to depend on the saturation of the metal's coordination sphere, since the trigonal planar compound **5** is twice as active as the tetrahedral one (compound **4**) against all bacteria strains. As for the interaction with CT DNA, it is found that the affinity of all the silver(I) complexes is high and takes place via an intercalative mode.

APPENDIX A. Supplementary data

CCDC 1824945-1824949 contain the supplementary crystallographic data for compounds **1-5**. These data can be obtained free of charge via <http://www.ccdc.cam.ac.uk/conts/retrieving.html>, or from the Cambridge Crystallographic Data Centre, 12 Union Road, Cambridge CB2 1EZ, UK; fax: (+44) 1223-336-033; or e-mail: deposit@ccdc.cam.ac.uk. Additional plots for CT DNA interaction studies with thioamide ligands and complexes **1-5** (Fig. **S1-S4**).

REFERENCES

- [1] (a) E.S. Raper, *Coord. Chem. Rev.* 129 (1994) 91-156; (b) E.S. Raper, *Coord. Chem. Rev.* 153 (1996) 199-255; (c) E.S. Raper, *Coord. Chem. Rev.* 165 (1997) 475-567.
- [2] (a) S.K. Hadjikakou, P. Aslanidis, P. Karagiannidis, D. Mentzafos, A. Terzis, *Inorg. Chim. Acta* 186 (1991) 199-204; (b) S.K. Hadjikakou, P. Aslanidis, P. Karagiannidis, A. Aubry, S. Skoulika, *Inorg. Chim. Acta* 193 (1992) 129-135; (c) D. Anastasiadou, G. Psomas, M. Lalia-Kantouri, A.G. Hatzidimitriou, P. Aslanidis, *Mater. Sci. Eng. C* 68 (2016) 241-250; (d) F. Karasmani, A. Tsipis, P. Angaridis, A.G. Hatzidimitriou, P. Aslanidis, *Inorg. Chim. Acta* 471 (2018) 680-690.
- [3] (a) K.D. Karlin, J. Zubieta, *Copper Coordination Chemistry: Biochemical and Inorganic Perspectives*, Adenine Press, New York, 1983; (b) B. Krebs, G. Henkel, *Angew. Chem. Int. Ed. Engl.* 30 (1991) 769-788.
- [4] For example: (a) S. Braun, A. Botzki, S. Salmen, C. Textor, G. Bernhardt, S. Dove, A. Buschauer, *Eur. J. Med. Chem.* 46 (2011) 4419-4429; (b) Y. Liu, J. Wu, P.-Y. Ho, L.-C. Chen, C.-T. Chen, Y.-C. Liang, C.-K. Cheng, W.-S. Lee, *Cancer Letters* 271 (2008) 294-305; (c) C.-R. Shih, J. Wu, Y. Liu, Y.-C. Liang, S.-Y. Lin, M.-T. Sheu, W.-S. Lee,

- Biochem. Pharmacol. 67 (2004) 67-75; (d) C. Congiu, M.T. Cocco, V. Omnis, Bioorg. Med. Chem. Lett. 18 (2008) 989-993.
- [5] (a) I. Tsyba, B.-k. Mui, R. Bau, R. Noguchi, K. Nomiya, Inorg. Chem. 42 (2003) 8028-8032; (b) K. Nomiya, K. Tsuda, N.C. Kasuga, J. Chem. Soc., Dalton Trans., 1998, 1653-1659; (c) M.I. Azócar, G. Gómez, C. Velásquez, R. Abarca, M.J. Kogan, M. Páez, Mater. Sci. Eng. C 37 (2014) 356-362, and references therein
- [6] (a) P.C. Zachariadis, S.K. Hadjidakou, N. Hadjiliadis, S. Skoulika, A. Michaelides, J. Balzarini, E.D. Clercq, Eur. J. Inorg. Chem., 2004, 1420-1426; (b) S.K. Hadjidakou, I.I. Ozturk, M.N. Xanthopoulou, P.C. Zachariadis, S. Zartilas, S. Karkabounas, N. Hadjiliadis, J. Inorg. Biochem., 102 (2008) 1007-1015; (c) C.N. Banti, A.D. Giannoulis, N. Kourkoumelis, A.M. Owczarzak, M. Poyraz, M. Kubicki, K. Charalabopoulos, S.K. Hadjidakou, Metallomics, 4 (2012) 545-560; (d) M.L. Teyssot, A.S. Jarrousse, M. Manin, A. Chevy, S. Roche, F. Norre, C. Beaudoin, L. Morel, D. Boyer, R. Mahiou, A. Gautier, Dalton Trans., 2009, 6894-6902; (e) B. Biersack, A. Ahmad, F.H. Sarkar, R. Schobert, Curr. Med. Chem., 19 (2012) 3949-3956; (f) A. Gautier, F. Cisnetti, Metallomics, 4 (2012) 23-32; (g) W. Liu, R. Gust, Chem. Soc. Rev., 42 (2013) 755-773.
- [7] C.N. Banti, S.K. Hadjidakou, Metallomics, 5 (2013) 569-596.
- [8] (a) P. Karagiannidis, P. Aslanidis, S. Kokkou, C.J. Cheer, Inorg. Chim. Acta 172 (1990) 247-251; (b) P. Aslanidis, P. Karagiannidis, P.D. Akrivos, B. Krebs, M. Läge, Inorg. Chim. Acta 254 (1997) 277-284; (c) W. McFarlane, P.D. Akrivos, P. Aslanidis, P. Karagiannidis, C. Hatzisymeon, M. Numan, S. Kokkou, Inorg. Chim. Acta 281 (1998) 121-125.
- [9] P.J. Cox, P. Aslanidis, P. Karagiannidis, S. Hadjidakou, Inorg. Chim. Acta 310 (2000) 268-272.

- [10] M.A. Tsiaggali, E.G. Andreadou, A.G. Hatzidimitriou, A.A. Pantazaki, P. Aslanidis, J. Inorg. Biochem. 121 (2013) 121-128.
- [11] O. Evangelinou, A.G. Hatzidimitriou, E. Velali, A.A. Pantazaki, N. Voulgarakis, P. Aslanidis, Polyhedron 72 (2014) 122-129.
- [12] (a) P. Aslanidis, A.G. Hatzidimitriou, E.G. Andreadou, A.A. Pantazaki, N. Voulgarakis, Mat. Sci. Eng. C 50 (2015) 187-193; (b) P. A. Papanikolaou, A. G. Papadopoulos, E. G. Andreadou, A. Hatzidimitriou, P. J. Cox, A. A. Pantazaki, P. Aslanidis, New J. Chem. 2015, 39, 4830-4844
- [13] J. Marmur, J. Mol. Biol. 3 (1961) 208-211. J. Marmur, J. Mol. Biol. 3 (1961) 208-211.
- [14] M.F. Reichmann, S.A. Rice, C.A. Thomas, P. Doty, J. Am. Chem. Soc. 76 (1954) 3047-3053.
- [15] Bruker Analytical X-ray Systems, Inc., 2006. Apex2, Version 2 User Manual, M86-E01078, Madison, WI.
- [16] P. W. Betteridge, J. R. Carruthers, R. I. Cooper, K. Prout, D. J. J. Watkin, Appl. Cryst. 36 (2003) 1487.
- [17] L. J. Farrugia, J. Appl. Cryst. 45 (2012) 849.
- [18] A. Wolfe, G. Shimer, T. Meehan, Biochemistry 26 (1987) 6392-6396..
- [19] J.R. Lakowicz, Principles of Fluorescence Spectroscopy, 3rd ed., Plenum Press, New York, (2006). J.R. Lakowicz, Principles of Fluorescence Spectroscopy, 3rd ed., Plenum Press, New York, (2006).
- [20] G. Zhao, H. Lin, S. Zhu, H. Sun, Y. Chen, J. Inorg. Biochem. 70 (1998) 219-226.
- [21] D.P. Heller, C.L. Greenstock, Biophys. Chem. 50 (1994) 305-312.
- [22] M.A. Tsiaggali, E.G. Andreadou, A.G. Hatzidimitriou, A.A. Pantazaki, P. Aslanidis, J. Inorg. Biochem. 121 (2013) 121-128.
- [23] A. C. Fabretti, A. Giusti, Polyhedron 5 (1986) 1927-1930.

-
- [24] B.M. Zeglis, V.C. Pierre, J.K. Barton, *Chem. Commun.* (2007) 4565-4579. B.M. Zeglis, V.C. Pierre, J.K. Barton, *Chem. Commun.* (2007) 4565-4579.
- [25] G. Pratviel, J. Bernadou, B. Meunier, *Adv. Inorg. Chem.* 45 (1998) 251-262.
- [26] A.M. Pyle, J.P. Rehmman, R. Meshoyrer, C.V. Kumar, N.J. Turro, J.K. Barton, *J. Am. Chem. Soc.* 111 (1989) 3051-3058.
- [27] Y. Wang, H. Zhang, G. Zhang, W. Tao, S. Tang, *J. Luminescence* 126 (2007) 211-218.
- [28] A. Dimitrakopoulou, C. Dendrinou-Samara, A.A. Pantazaki, M. Alexiou, E. Nordlander, D.P. Kessissoglou, *J. Inorg. Biochem.* 102 (2008) 618-628.
- [29] J.L. Garcia-Gimenez, M. Gonzalez-Alvarez, M. Liu-Gonzalez, B. Macias, J. Borrás, G. Alzuet, *J. Inorg. Biochem.* 103 (2009) 923-934. J.L. Garcia-Gimenez, M. Gonzalez-Alvarez, M. Liu-Gonzalez, B. Macias, J. Borrás, G. Alzuet, *J. Inorg. Biochem.* 103 (2009) 923-934.
- [30] W.D. Wilson, L. Ratmeyer, M. Zhao, L. Streckowski, D. Boykin, *Biochemistry* 32 (1993) 4098-4104.

